Monthly Notices
of the
ROYAL ASTRONOMICAL SOCIETY

Mon. Not. R. Astron. Soc. **416,** 2857–2868 (2011) doi:10.1111/j.1365-2966.2011.19234.x

3C 390.3: more stable evidence that the double-peaked broad Balmer lines originate from an accretion disc near a central black hole

Xue-Guang Zhang[1,2]★

[1]*Purple Mountain Observatory, Chinese Academy of Sciences, 2 Beijing XiLu, Nanjing, Jiangsu, 210008, China*
[2]*Department of Physics and Astronomy, Texas A&M University, College Station, Texas, 77843-4242, USA*

Accepted 2011 June 13. Received 2011 May 3; in original form 2011 February 1

ABSTRACT

In this paper, we study the structure of the broad emission-line regions (BLRs) of the well-known double-peaked emitter (an active galactic nucleus with broad double-peaked low-ionization emission lines) 3C 390.3. Besides the best-fitting results for the double-peaked broad optical Balmer lines of 3C 390.3 obtained from the theoretical disc model, we also try to find another way to further confirm that the double-peaked line originates from an accretion disc. Based on the long-period spectra in the optical band observed around 1995, collected by the AGN Watch project, the theoretical disc parameters of disc-like BLRs supposed by the elliptical accretion disc model have been well determined. Using theoretical disc-like BLRs, the characteristics of the observed light curves of the broad double-peaked Hα of 3C 390.3 can be reproduced well, based on the reverberation mapping technique. Thus, the accretion disc model is preferred as the better model for the BLRs of 3C 390.3. Furthermore, we find that different disc parameters should lead to some different results about the size of the BLRs of 3C 390.3 from those measured using observational data. This indicates that the measured disc parameters are valid for 3C 390.3. After this, with the precession of theoretical elliptical disc-like BLRs considered, we find that the line profile in 2000 expected by the theoretical model is consistent with the line profile observed by the *Hubble Space Telescope* around 2000. Based on the results, we believe that the broad double-peaked Balmer emission lines of 3C 390.3 originate from an accretion disc around a central black hole.

Key words: galaxies: active – galaxies: individual: 3C 390.3 – galaxies: nuclei – quasars: emission lines – galaxies: Seyfert.

1 INTRODUCTION

The properties of objects with broad double-peaked low-ionization emission lines (double-peaked emitters hereafter) have been studied for more than two decades, since double-peaked emitters were found in nearby radio galaxies (Stauffer, Schild & Keel 1983; Oke 1987; Perez et al. 1988; Chen & Halpern 1989; Chen, Halpern & Filippenko 1989; Halpern 1990). Some theoretical models have been proposed to explain the properties of double-peaked broad emission lines, which can be used to probe the broad-line regions of active galactic nuclei (AGNs; Eracleous, Lewis & Flohic 2009); for example, the binary black hole (BH) model (Begelman, Blandford & Rees 1980; Gaskell 1983, 1996; Zhang, Dultzin & Wang 2007; Boroson & Lauer 2009; Lauer & Boroson 2009), the double-stream model (Zheng, Sulentic & Binette 1990; Veilleux & Zheng 1991; Zheng, Veilleux & Grandi 1991), the accretion disc model (Chen & Halpern 1989; Chen et al. 1989; Eracleous et al. 1995, 1997; Bachev 1999; Hartnoll & Blackman 2000, 2002; Karas, Martocchia & Subr 2001; Gezari, Halpern & Eracleous 2007; Flohic & Eracleous 2008; Chornock et al. 2010; Gaskell 2010; Lewis, Eracleous & Storchi-Bergmann 2010; Tran 2010) etc. Although it is still under debate which theoretical model is preferable for double-peaked emitters, the accretion disc model, which indicates that double-peaked broad emission lines are from a central accretion disc, is so far the more widely accepted model applied to explain the properties of double-peaked broad emission lines.

Because of the unobscured emitting region on the receding jet, the double-stream model can be ruled out for double-peaked emitter 3C 390.3 (Livio & Xu 1997). Using long-period observational results, the binary BH model has also been ruled out, because of the unreasonably large central BH masses for some double-peaked emitters, such as Arp102B, 3C 390.3 (Eracleous et al. 1997). Furthermore, based on the long-period variations of double-peaked broad emission lines, the accretion disc model is successfully applied to reproduce the characteristics of the varying observed line

★E-mail: xgzhang@pmo.ac.cn

profiles of double-peaked emitters, such as the individual double-peaked emitter NGC 1097 (Storchi-Bergmann et al. 1995, 1997, 2003), and one sample of double-peaked emitters (Gezari et al. 2007; Lewis et al. 2010). However, we should note that although the accretion disc model is so far the widely accepted theoretical model for double-peaked emitters, other theoretical models are expected to be preferred for some special double-peaked emitters, such as x-shaped radio objects, which could be candidates for objects with binary BHs in central regions (Merritt & Ekers 2002; Zhang et al. 2007). Thus, based only on the double-peaked appearance of broad emission lines, there is no confirmed way to affirm which theoretical model is more preferred for double-peaked emitters.

Among the reported double-peaked emitters (Eracleous & Halpern 1994, 2003; Eracleous et al. 1995; Strateva et al. 2003), 3C 390.3 is a well-studied double-peaked emitter, and also one well-studied mapping AGN (Leighly et al. 1997; Dietrich et al. 1998; O'Brien et al. 1998; Shapovalova et al. 2001, 2010; Sergeev et al. 2002; Peterson et al. 2004; Pronik & Sergeev 2007; Sambruna et al. 2009; Jovanovic et al. 2010). Based on the reverberation mapping technique (Blandford & Mckee 1982) and virialization method (Peterson et al. 2004; Collin et al. 2006; Peterson & Bentz 2006; Peterson 2010), the sizes of BLRs (the distance between the central BH and the broad line emission gas clouds) and central virial BH masses of 3C 390.3 have been well determined (Onken et al. 2004; Peterson et al. 2004; Kaspi et al. 2005; Bentz et al. 2006, 2009; Brandon & Bechtold 2007). Besides the common BH masses and sizes of BLRs, using the theoretical accretion disc model applied to observed double-peaked broad emission lines, some basic disc parameters of the supposed theoretical disc-like BLRs of 3C 390.3 have also been measured (Eracleous & Halpern 1994), such as the inclination angle of the accretion disc, the inner and outer radii of the BLRs in the accretion disc, etc. However, because of the best-fitting results for double-peaked Balmer lines using the accretion disc model, we cannot definitely confirm that the double-peaked broad emission lines come exactly from the disc-like BLRs in the accretion disc around the central BH for 3C 390.3.

Besides the best-fitting results for the double-peaked broad emission lines using theoretical models, based on the pioneer work of Blandford & Mckee (1982), the geometrical structures of BLRs can be mathematically structured by the so-called transfer function in the reverberation mapping technique using some special mathematical methods (such as the maximum Entropy method; Narayan & Nityananda 1986) applied to the properties of long-period observations, varying both continuum emission and broad-line emission (Horne, Welsh & Peterson 1991; Goad, O'Brien & Gondhalekar 1993; Peterson et al. 1993, 1994; Krolik 1994; Pijpers & Wanders 1994; Wanders & Horne 1994; Winge et al. 1995; Bentz et al. 2010). However, it is unfortunate that there is no unique solution to the so-called transfer function used to determine the structures of the BLRs of AGNs, because of the less complete information about the variations in continuum and broad emission lines (Maoz 1996). Thus, even based on the solution of the transfer function, the supposed theoretical and mathematical geometrical structures of the BLRs of AGNs cannot yet be firmly confirmed.

In previous work studying the structures of the BLRs of AGNs, the main objective has been to determine the structures of BLRs through observational properties/characteristics. However, we think it would also be very interesting to check whether the observational properties of the long-period variations of broad-line emission and/or continuum emission could be better reproduced through the reverberation mapping technique, based on the expected structures of the BLRs supposed by the theoretical model. This is the main objective of our paper.

The structure of our paper is as follows. In Section 2 we give some information on the spectra of 3C 390.3 observed around 1995. We discuss how to find the theoretical disc parameters for the supposed disc-like BLRs using the best-fitting results for the broad double-peaked Balmer lines from the theoretical elliptical accretion disc model (Eracleous et al. 1995). In Section 3 we show the results of the reverberation mapping technique under the disc-like BLRs for 3C 390.3. Finally, in Section 4 we provide a detailed discussion and some conclusions. The cosmological parameters $H_0 = 70\,\mathrm{km\,s^{-1}\,Mpc^{-1}}$, $\Omega_\Lambda = 0.7$ and $\Omega_\mathrm{m} = 0.3$ have been adopted here.

2 FITTED RESULTS FOR THE SPECTRA OF 3C 390.3 AROUND 1995

As one well-known double-peaked broad line AGN, 3C 390.3 ($z = 0.056$) is one target included in the project of AGN Watch (http://www.astronomy.ohio-state.edu/∼agnwatch/). This is a consortium of astronomers who have studied the inner structure of AGNs through continuum and emission-line variability. From the AGN Watch project, we can collect 133 spectra of 3C 390.3 in the optical band, observed around 1995 by different instruments at different observatories. Meanwhile, the light curves of the continuum and broad emission lines, after necessary corrections for some contamination, are also collected from the website. Detailed descriptions about the instruments and techniques for the observed spectra can be found in Dietrich et al. (1998). Here, we do not describe the information any further. We mainly focus on how to determine the disc parameters using the theoretical accretion disc model for 3C 390.3.

In order to obtain reliable disc parameters for the disc-like BLRs of 3C 390.3, which as supposed by the theoretical accretion disc model are applied to fit the double-peaked broad emission lines, we prefer to use the double-peaked broad Hα rather than the double-peaked broad Hβ. This is because of the more apparent double peaks of broad Hα (one peak of the double-peaked broad Hβ is mixed by the [O III]λ4959, 5007 Å doublet) and the stronger broad Hα than broad Hβ. Thus, we mainly focus on the 66 of the 133 observed spectra that have reliable broad Hα within a rest wavelength from 6200 to 7300 Å.

So far, there are several types of accretion disc models that can be applied to double-peaked emitters: a circular accretion disc model with/without spiral arms (Chen et al. 1989; Chen & Halpern 1989; Hartnoll & Blackman 2002), an elliptical accretion disc model (Eracleous et al. 1995), a warped accretion disc model (Hartnoll & Blackman 2000), a stochastically perturbed accretion disc model (Flohic & Eracleous 2008) etc. In this paper, the elliptical accretion disc model (Eracleous et al. 1995) is preferred, because this model can explain most of the observational spectral features of broad double-peaked emission lines (especially features for extended asymmetric line wings) with fewer necessary model parameters. Furthermore, most of the flux density of the broad double-peaked line emission is from disc-like BLRs into the accretion disc. The existence of arms (Hartnoll & Blackman 2002) and/or warped structures (Hartnoll & Blackman 2000) and/or bright spots (Flohic & Eracleous 2008) is mainly applied to subtle structures of double-peaked line profiles (such as some cusps around the peaks, etc.). These have few effects on the results based on the cross-correlation function (CCF) in the reverberation mapping technique. A detailed description of the elliptical accretion disc model with seven model parameters can be found in Eracleous et al. (1995).

The seven necessary parameters are the inner radius r_0, the outer radius r_1, the eccentricity of the elliptical rings e, the local broadening velocity σ, the inclination angle of the disc-like BLRs i, the line emissivity slope ($f_r \propto r^{-q}$) and the orientation angle of the elliptical rings ϕ_0. Using the Levenberg–Marquardt least-squares minimization method to fit the double-peaked broad Hα with the elliptical accretion disc model, as we have done for the x-shaped radio source SDSS J1130+0058 (Zhang et al. 2007), the seven disc parameters in the elliptical accretion disc model can be determined well. The procedures to determine the disc parameters for the BLRs of 3C 390.3 are as follows.

First and foremost, in order to check the results from the reverberation mapping technique under the structures of BLRs supposed by the accretion disc model, we should measure reliable theoretical disc parameters for the disc-like BLRs of 3C 390.3. Before starting to fit the observed broad double-peaked Hα, we first check the spectra of 3C 390.3 by eye. We find that the spectra marked with 'ce' (the corresponding observatory can be found in table 1 of Dietrich et al. 1998) have some unexpected absorption features around 6500 Å in the rest wavelength. The weird absorption features cannot be found in other spectra observed by instruments at other observatories. This should create some larger uncertainties in the measured disc parameters when broad Hα is fitted by the accretion disc model. Thus, the absorption features (rest wavelength from 6507 to 6525 Å) in the 24 spectra marked with 'ce' should be rejected, when broad Hα is fitted by the elliptical accretion disc model for 3C 390.3. Besides the weird absorption features in the 24 spectra marked with 'ce', in order to reduce the effects of narrow emission lines ([O I]λ6300, 6363 Å, [N II]λ6548, 6583 Å, [S II]λ6716, 6731 Å and narrow Hα) in all the spectra, parts of the narrow emission lines are also masked when broad Hα is fitted: rest wavelength from 6268 to 6326 Å for [O I]λ6300 Å, rest wavelength from 6350 to 6388 Å for [O I]λ6363 Å, rest wavelength from 6533 to 6619 Å for [N II]λ6548, 6583 Å and narrow Hα, rest wavelength from 6703 to 6743 Å for [S II]λ6716, 6731 Å (the grey shading shown in Figs 1, 2 and 5). In other words, only the double-peaked broad components of Hα without weird absorption features and without narrow emission lines are fitted. After this preparation, the double-peaked broad Hα is fitted twice as follows.

First, the 39 high-quality spectra (more than 280 reliable data points within the rest wavelength range from 6160 to 6920 Å) without unexpected absorption features around 6500 Å are fitted by the elliptical accretion disc model. Then, using the measured disc parameters, the two parameters of eccentricity and inclination angle are first determined for the 39 spectra, because eccentricity and inclination angle should not be changed with the passage of time. The mean values of the two parameters for the 39 spectra are accepted as the reliable values for the two parameters. Then, all 66 spectra are fitted again by the accretion disc model with the accepted constant inclination angle and eccentricity. Fig. 1 shows the best-fitting results for some selected broad Hα by the elliptical accretion disc model with MJD from 49770 to 50051. In the figure, two spectra with unexpected absorption features (marked by '49860ce' and '49984ce') are also shown; the shaded areas represent the masked ranges for the narrow emission lines. Fig. 2 shows the corresponding residuals ($y_{\rm obs} - y_{\rm model}$, observed data minus expected model data) for the examples shown in Fig. 1. In the figure, shaded areas represent the narrow emission lines. Each double horizontal dashed line represents the range $[f_0 - 1, f_0 + 1]$, where $f_0 = 0$, 10, 20...80, representing the zero-point for each spectrum shown as a solid horizontal line in the figure. The results shown in Figs 1 and 2 indicate that the elliptical disc model is better for the double-peaked

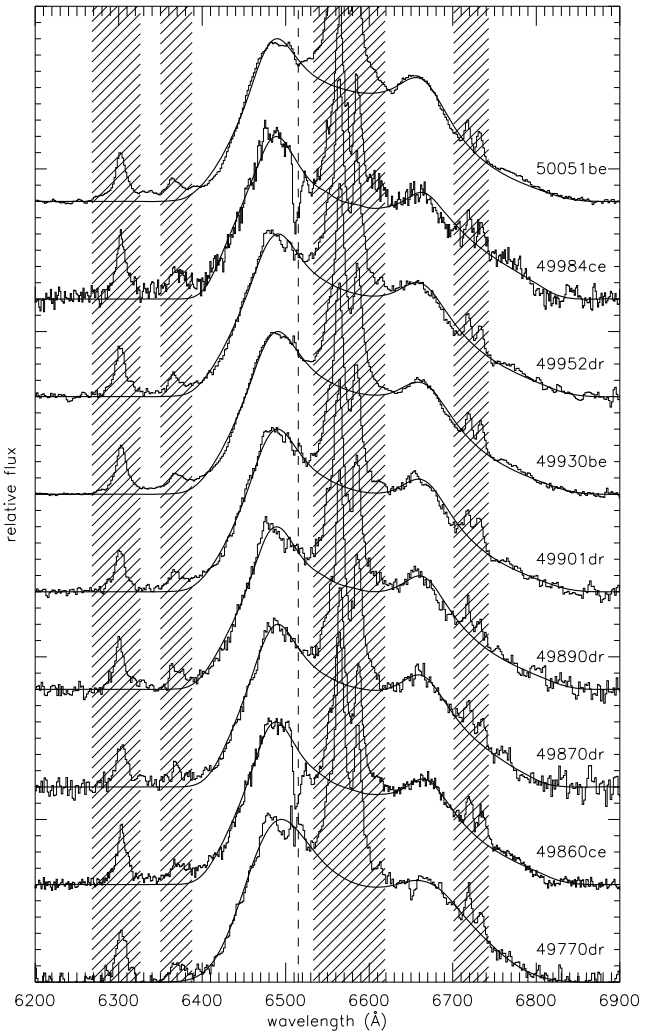

Figure 1. Best-fitting results for double-peaked broad Hα in the rest wavelength using the elliptical accretion disc model. The thin solid line represents the observed spectrum and the thick solid line represents the best-fitting results for double-peaked broad Hα. The vertical dashed line shows the position for unexpected absorption features around 6500 Å for two examples marked with '49860ce' and '49984ce'. The observed MJD date of each spectrum is shown on the right side of the figure. Shaded areas represent the ranges for narrow emission lines.

broad emission lines of 3C 390.3. The results further indicate that the probable existing hotspots and/or warped structures have few effects on the measured flux density of broad Hα and few effects on our final results and conclusions (i.e. the hotspots and/or ward structures are weak for the spectra of 3C 390.3 observed around 1995, and the elliptical accretion disc model is efficient and sufficient for 3C 390.3 around 1995).

Fig. 3 shows the distributions of the disc parameters, and the distributions of the parameter of $\log(\chi^2)$ (the value of the summed squared residuals divided by the degree of freedom for the returned model parameter values, which is one parameter as the residual to determine whether the theoretical model is preferred) for the 39 high-quality spectra in the upper three panels and for all 66 spectra in the other six panels. The final accepted disc parameters are the inner radius $r_0 = 216 \pm 26R_{\rm G}$, the outer radius $r_1 = 1263 \pm 70R_{\rm G}$, the eccentricity $e = 0.13 \pm 0.04$, the inclination angle $i = 29.57 \pm 1.67^\circ$, the orientation angle $\phi_0 = -23 \pm 7^\circ$, the emissivity power

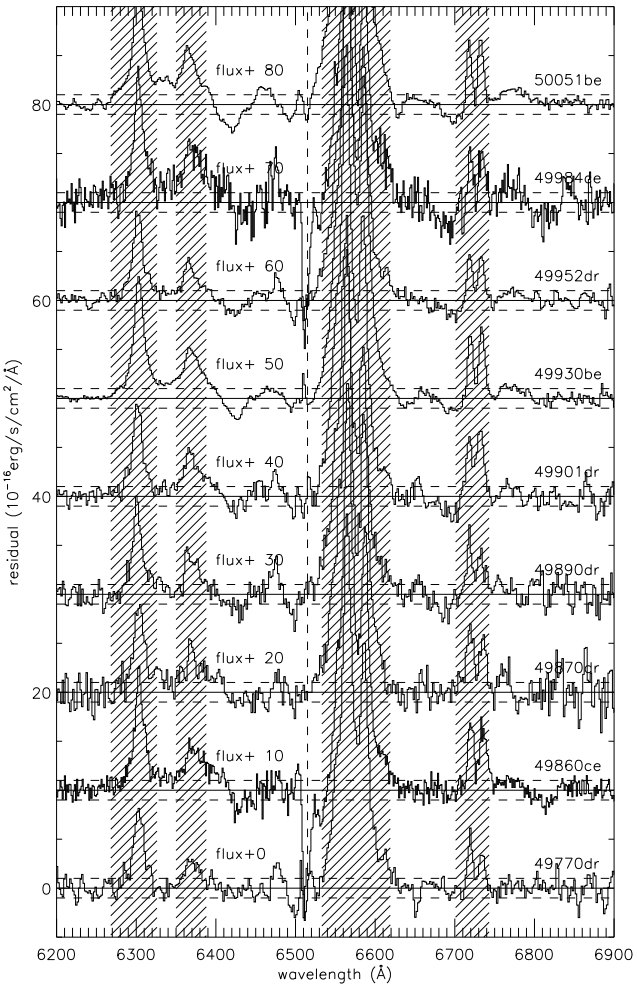

Figure 2. The residuals ($y_{\rm obs} - y_{\rm model}$, observed data minus expected model data) for the examples shown in Fig. 1. Shaded areas represent the ranges for narrow emission lines. Each double horizontal dashed line represents the range of $[f_0 - 1, f_0 + 1]$, where $f_0 = 0$, 10, 20...80, representing the zero-point for each spectrum, are shown as solid horizontal lines in the figure.

slope $q = 1.65 \pm 0.26$ [$f(r) \propto r^{-q}$] and the local broadening velocity $\sigma = 742 \pm 145\,{\rm km\,s^{-1}}$. Actually, we should note that some of the theoretical disc parameters, r_0, r_1, q, ϕ_0 and σ, should depend on the strength of continuum emission; in other words, the parameters are time-dependent. However, there should be long-term progressive changes in the ionizing flux to change these variables. Moreover, from the results shown in Fig. 3, we find that there are tiny variations for these parameters. This indicates that the mean values for the theoretical disc parameters can be used to trace the actual physical disc parameters for 3C 390.3 around 1995.

Before proceeding further, we compare our measured disc parameters with the previous results reported in the literature. In the sample of double-peaked emitters from radio galaxies, Eracleous & Halpern (1994) gave the results of disc parameters for BLRs using the circular accretion disc model (Chen et al. 1989) for double-peaked broad Hα observed in 1988 for 3C 390.3 (simple results can also be found in Fig. 6 and in section 4.5 of Sambruna et al. 2009). These are different from our results determined using the elliptical accretion disc model (Eracleous et al. 1995). We know that in the accretion disc model, the full width at zero intensity (FWZI) of the double-peaked broad emission lines sensitively depends on the inner radius of the disc-like BLRs, and a smaller inner radius leads to a broader FWZI. From the fitted results shown in fig. 4 of Eracleous & Halpern (1994), we find that in order to better fit the broad wings of broad Hα, the inner radius should be smaller than $380R_{\rm G}$ (i.e. that listed in Eracleous & Halpern 1994). Thus, our inner radius $r_0 = 216R_{\rm G}$ should be reasonable. The peak separation sensitively depends on the outer radius, and thus there are similar results for the outer radius in Eracleous & Halpern (1994) and in our paper. In order to better fit the cusp feature around the blue peak, the elliptical disc model should be more efficient than the totally symmetric circular disc model (i.e. the parameters of eccentricity and orientation angle should be active). The separation between the peak intensity and zero intensity of the blue (or red) part of Hα should depend on the emissivity power slope. The larger distance between our inner radius and outer radius indicates that our emissivity slope should be smaller than 3 (i.e. that listed in Eracleous & Halpern 1994). Thus, our emissivity slope $q = 1.65$ should be reasonable. The linewidth of the double-peaked broad line sensitively depends on the inclination angle. Thus, it is clear that there are similar values of the inclination angle $i \sim 30^\circ$ in our paper and in Eracleous & Halpern (1994). Because the elliptical accretion disc model is more efficient for 3C 390.3 than the circular accretion disc model, the effects from the local broadening velocity should be lower. Thus, our local broadening velocity $\sigma \sim 750\,{\rm km\,s^{-1}}$, which is smaller than $1900\,{\rm km\,s^{-1}}$ in Eracleous & Halpern (1994), should be reasonable.

Besides the disc parameters, it is interesting to check the variations of the line profiles of the double-peaked broad Hα. As shown in Veilleux & Zheng (1991), there are significant variations of the relative flux ratio of the two peaks within the period from 1974 to 1988. Certainly, the variations cannot be successfully explained by the elliptical accretion disc model, because the disc precession period of 3C 390.3, based on the elliptical accretion disc model, is about several hundreds of years, as we discuss in the following. However, during the period (about 500 d) around 1995 included in the AGN Watch project, the variations of flux ratio of the two peaks are tiny, as shown in Fig. 4. In the figure, two types of flux ratio are shown: the one with the mean value of 1.01 ± 0.02 (0.02 is the standard deviation for the mean value) is the ratio of the blue part to the red part of broad Hα divided by 6564.61 Å (the theoretical centre wavelength of Hα); the other with the mean value of 1.46 ± 0.06 (0.06 is the standard deviation) is the intensity ratio of the blue peak to the red peak. Similar results for 3C 390.3 around 1995 can also be found in Dietrich et al. (1998). More recent results for the flux ratio of the two peaks of 3C 390.3 from 1995 to 2007 can be found in Shapovalova et al. (2010). There are tiny variations of the flux ratio of the two peaks in the 5-yr period, as shown in fig. 13 of Shapovalova et al. (2010). Because of these tiny variations, we believe that there are tiny variations for the disc parameters obtained from the spectra observed during 1995, and this is the reason why we select the spectra observed around 1995. In other words, the structures of the BLRs of 3C 390.3 are stable around 1995, which confirms that there are tiny variations of the disc parameters shown in Fig. 3.

Last but not least, we should note that the 66 spectra collected in the optical band for 3C 390.3 are the spectra observed before the intercalibration method (van Groningen & Wanders 1992) was applied to consider the effects from different observational instruments in different configurations, as discussed in Dietrich et al. (1998). In this paper, we mainly focus on the disc parameters, rather than the flux densities of broad Hα, which should be directly collected from

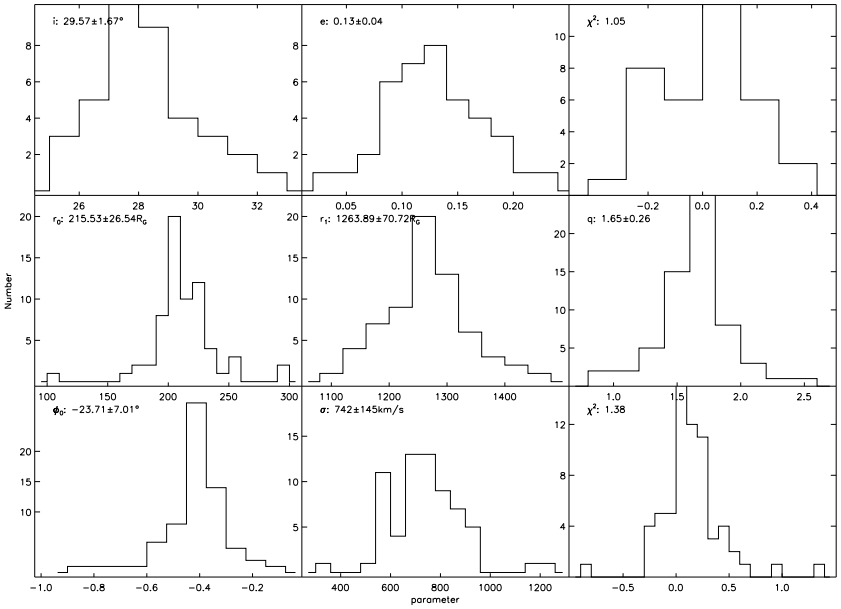

Figure 3. Distributions of the disc parameters of disc-like BLRs for 3C 390.3. The top three plots show the distributions of eccentricity, inclination angle and the parameter of $\log(\chi^2)$ for the 39 spectra with high quality and without unexpected absorption features around 6500 Å. Then, the other six plots show the distributions of the other parameters for all 66 spectra, the inner radius r_0, the outer radius r_1, the emissivity slope q, the orientation angle ϕ_0, the local broadening velocity σ and the parameter of $\log(\chi^2)$. The mean value of each parameter we accepted is shown in each plot.

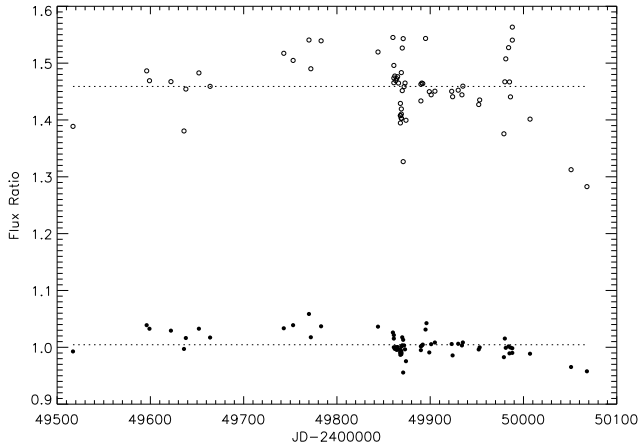

Figure 4. The variations of the flux ratio of blue peak to red peak (shown as open circles), and the flux ratio of blue part to red part of broad Hα (shown as solid circles). The dotted lines represent the mean values of the two types of flux ratio.

the AGN Watch project with the contamination corrected. The main effect of the intercalibration method on the corrected line profile is the broadening velocity in the method. However, the broadening velocity is only about tens of kilometres per second when the intercalibration method is applied, which is much smaller than the linewidth of broad Hα. Thus, the effects of the intercalibration method on the measured disc parameters using the elliptical accretion disc model can be totally ignored.

Before finishing this section, we consider whether there are other values for the disc parameters in the disc model that can be applied to fit the observed double-peaked broad Hα well. In other words, the question is whether the solutions to the disc parameters are unique. If the answer is yes, there should be one set of values for the disc parameters in the following mathematical procedure. We try to determine whether our mathematical procedure can be applied to determine the available parameter space. If the answer is no, the following mathematical procedure should be simple and succinct. To give one precise mathematical solution to the question is very difficult. We consider the question as follows. The observed double-peaked broad Hα is refitted. When the procedure starts to fit the line profile, one of the disc parameters is fixed to a value very different from the accepted value above (half of the accepted value for the parameter), and the other disc parameters with the same starting values in the fitting procedure are free. Then, the Levenberg–Marquardt least-squares minimization technique is applied to find the best-fitting results for the observed double-peaked broad Hα and we find the best solutions for the disc parameters. Actually, the software package MPFIT in the Markwardt IDL library[1] is used to perform the least-squares fitting and to find the best solution. In order to clearly compare the fitted results for different disc parameters, the value $flux_{fit1-fit2}$ is calculated. Here, $fit2$ denotes the best-fitting results for the accepted disc parameters shown in Fig. 3 and $fit1$ denotes the best-fitting results for one fixed disc parameter with half of the accepted value for the parameter. Fig. 5 shows the fitted results, and the corresponding values of $flux_{fit1-fit2}$. The apparent and large difference (residual to some extent) between $fit1$ and $fit2$ indicates that the solutions to the disc parameters based on the accretion disc model are unique to some extent. Thus, in the following mathematical procedure to determine the geometrical structure of the emission-line regions, there are fixed disc parameters.

Based on the results above, using the disc parameters, one type of disc-like geometrical structure of the BLRs of 3C 390.3 can be well structured. Then, it is very interesting to check whether the characteristics of the observed light curves can be reproduced using the theoretical disc-like BLRs of 3C 390.3. This is the main objective of the following section.

[1] See http://cow.physics.wisc.edu/~craigm/idl/

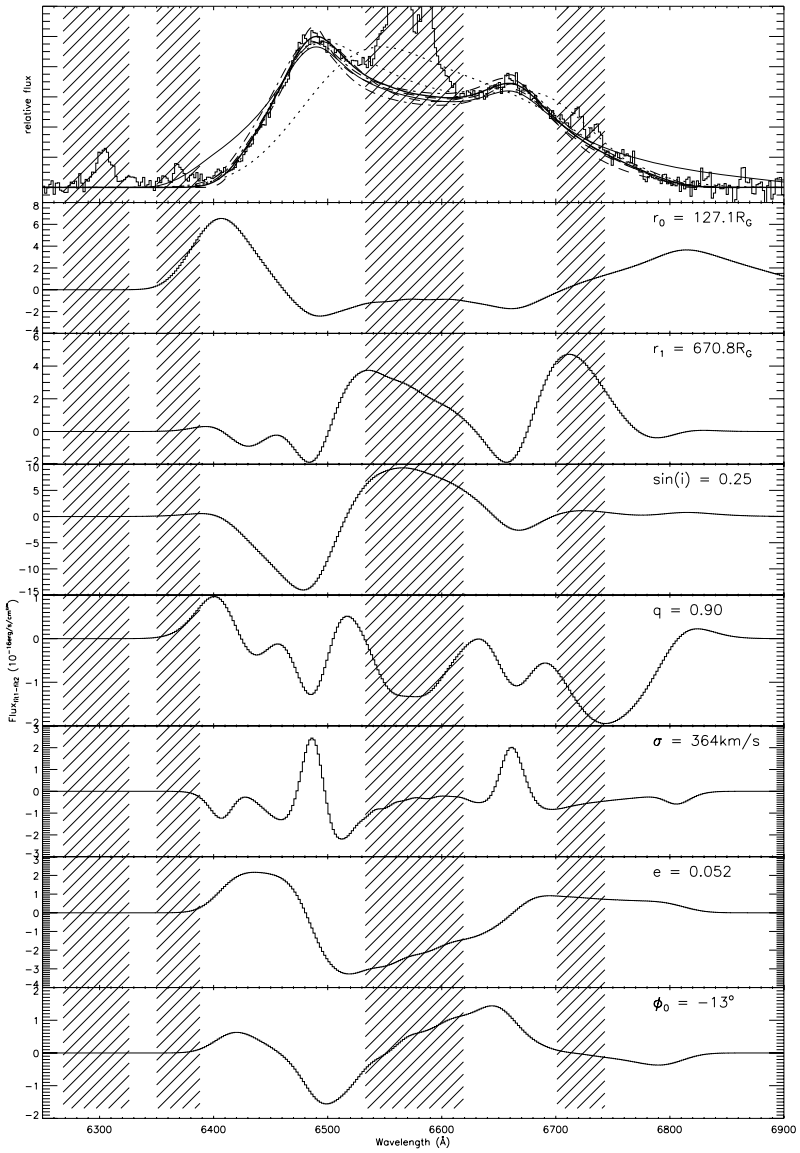

Figure 5. Best-fitting results for double-peaked broad Hα with one fixed parameter with half of the accepted value for the disc parameter. In the top panel, the thin solid line as a histogram represents the observed line profile marked with '49870dr' in the AGN Watch project. The thick solid line shows the best-fitting results, with the disc parameters having the values shown in Fig. 3. The thin solid line represents the best-fitting results with the disc parameter $r_0 = 127.1R_G$. The thin dotted line represents the best-fitting results with the disc parameter $r_1 = 670.8R_G$. The thick dotted line represents the best-fitting results with the disc parameter $\sin(i) = 0.25$. The thin dashed line represents the best-fitting results with the disc parameter $q = 0.90$. The thick dashed line represents the best-fitting results with the disc parameter $\sigma = 364\,\mathrm{km\,s^{-1}}$. The thin dot-dashed line represents the best-fitting results with the disc parameter $e = 0.052$. The thick dot-dashed line represents the best-fitting results with the disc parameter $\phi_0 = -13^\circ$. The other seven panels show the corresponding values of $flux_{fit1-fit2}$, where *fit*2 represents the best-fitting results with the disc parameters shown in Fig. 3.

3 RESULTS OF THE REVERBERATION MAPPING TECHNIQUE UNDER THE ELLIPTICAL ACCRETION DISC MODEL

In the previous section, one type of geometric structure of the BLRs of 3C 390.3 was supposed by the theoretical elliptical accretion disc model (Eracleous et al. 1995). In this section, we check whether the supposed disc-like BLRs are valid to reproduce the properties of the observed continuum and broad-line variability, using the reverberation mapping technique.

In order to clearly build one physical geometrical structure of disc-like BLRs, the length of one gravitational radius (R_G) in physical units should first be determined (i.e. it is necessary to determine the mass of the central BH of 3C 390.3). Here, the BH mass of 3C 390.3, $M_{BH} = 4.68 \times 10^8\ M_\odot$, is used. For 3C 390.3, the two types of BH mass, which are similar, both virial BH masses (Peterson et al. 2004) and BH masses from the M–σ relation (Gebhardt et al. 2000; Ferrarese & Merritt 2001; Tremaine et al. 2002; Lewis & Eracleous 2006; Göltekin et al. 2009; Woo et al. 2010) can be found in the literature. Thus, we do not worry about the accuracy of the BH masses of 3C 390.3, and we accept $R_G \sim 0.0263$ light-days based on the BH masses. Using the disc parameters above, it is not difficult to build the physical geometry of the BLRs of 3C 390.3 as supposed by the theoretical model. Then, it is interesting to check the results based on the reverberation mapping technique, using the supposed disc-like BLRs as follows.

First and foremost, we accept the assumptions listed in Peterson (1993) for the reverberation mapping technique. (i) The continuum emission is from one central source, which is much smaller than the BLRs. The assumption is efficient for 3C 390.3, although the double-peaked broad line of 3C 390.3 is assumed to be from the accretion disc. The reported size of the BLRs of 3C 390.3, the time lag between the observed optical Balmer emission and the observed ultraviolet (UV) X-ray emission, is about 20 ± 8 light-days (Dietrich et al. 1998; Bentz et al. 2009), i.e. $R_{\rm BLRs} \sim 400$–$1000R_{\rm G}$, using the CCF method. Based on the theoretical disc parameters for 3C 390.3, the flux-weighted mean size of the BLRs is about $567R_{\rm G}$ (simply calculated by $(r_0 + r_1)/(1. + q)$, where $q \sim 1.65$ is the line emissivity slope). The result indicates the UV emission region is much nearer to the central BH, which clearly can be treated as one point source. (ii) Both the continuum emission and line emission are freely and isotopically propagating in the central volume, which can be confirmed by the small covering factor estimated by the appearance of no-absorption features around broad Hα. (ii) The line emissions are in rapid response to the ionizing continuum, which can be confirmed by the strong correlation between line luminosity and continuum luminosity found by Greene & Ho (2005) and by the much shorter recombination time (about 100 s for standard BLRs) of the Balmer emission lines and the much longer dynamic time (about several years for standard BLRs) than the light travel time across BLRs, as discussed in Peterson (1993).

Moreover, we structure the supposed theoretical structures of the BLRs of 3C 390.3 as follows. More than 10^4 tiny clouds (or so-called test particles, if we treat each tiny cloud as a sufficient tiny size) are set in the N elliptical rings (the BLRs). Each tiny cloud has its position (radius r and orientation angle ϕ) and line intensity (f). The position in one elliptical ring for one tiny cloudy is created by

$$\phi \in [0, 2\pi]$$
$$r = \frac{r_\star(1+e)}{1 - e\cos(\phi)}. \quad (1)$$

Here, $r_0 \le r_\star \le r_1$ and e are the pericentre distance and eccentricity of the disc-like BLRs of 3C 390.3, respectively, and r is the distance from the tiny cloud to the central BH. From the inner boundary r_0 to the outer boundary r_1, the pericentre distance for the elliptical rings is evenly separated into N bins, $\log(r_0) \le \log[r_{\star,i}(i = 1 \ldots N)] \le \log(r_1)$ with steps of $[\log(r_1) - \log(r_0)]/(N-1)$. Because most of the line emission is from the inner area of the BLRs, the parameter of the logarithm of the pericentre distance $[\log(r)]$ is evenly separated, rather than the parameter of the pericentre distance (r), which provides more areas in the inner part of the BLRs. After this, the orientation angle ϕ is evenly separated into M bins, $0 \le \phi_j (j = 1 \ldots M) \le 2\pi$ with steps of $2\pi/(M-1)$. Based on $r_{\star,i}$ and ϕ_j, the supposed theoretical disc-like BLRs can be separated into $(N-1)(M-1)$ tiny areas $[A_{i,j}(i = 1 \ldots N, j = 1 \ldots M)]$. As long as N is large enough, the ionizing photopropagating time through each tiny area can be ignored, and each tiny cloud can be simply treated as one point source. The line intensity from each area

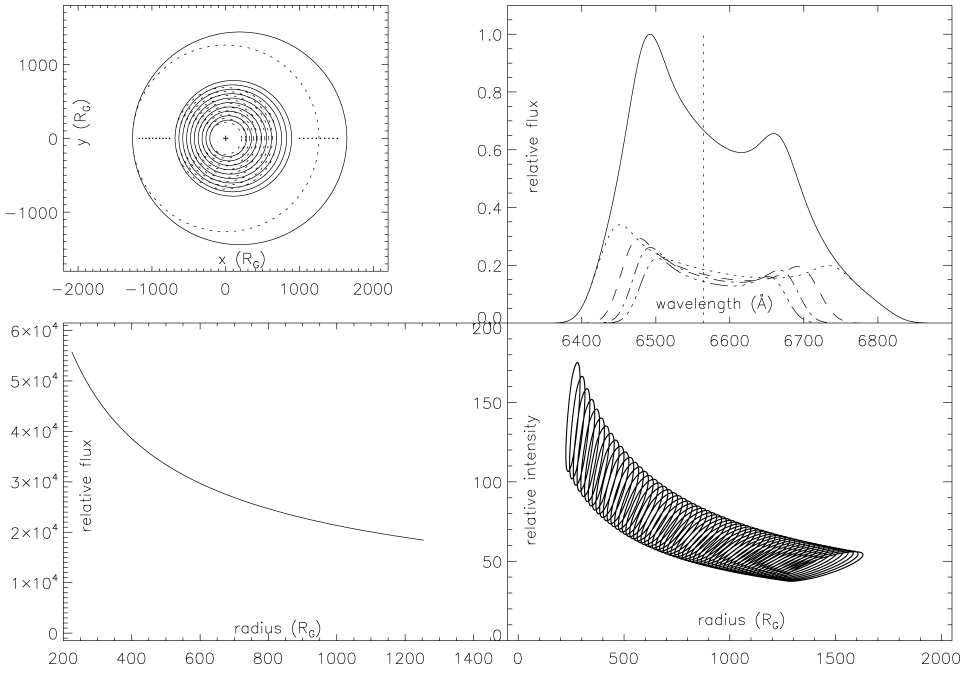

Figure 6. The top-left panel shows the structures of the elliptical disc-like BLRs of 3C 390.3. The solid line represents the elliptical ring with pericentre distance $r_0 \le r_i \le r_1$, the innermost with a pericentre distance of r_0 and the outermost with r_1. The central BH is located at the origin of the coordinates (one focus point of the elliptical ring). The dotted line represents the sphere surface of ionizing photons at one time. Because the BLRs are elliptical disc-like, at one time, the ionizing photons arriving in the BLRs do not affect all the tiny clouds located in one elliptical ring. The top-right panel shows the line intensity of broad Hα with different bins of radius. The solid line represents the observed Hα, the dotted line represents the line intensity from $\sim 216R_{\rm G}$ (the inner boundary) to $\sim 480R_{\rm G}$, the dashed line represents the line intensity from $\sim 480R_{\rm G}$ to $\sim 740R_{\rm G}$, the dot-dashed line represents the line intensity from $\sim 740R_{\rm G}$ to $\sim 1000R_{\rm G}$, and the double-dot-dashed line represents the line intensity from $\sim 1000R_{\rm G}$ to $1263R_{\rm G}$ (the outer boundary). The vertical dotted line represents the centre wavelength of Hα, 6564.61 Å. The bottom-left panel shows the correlation between line intensities from different bins $[F_i(r)]$ and the corresponding pericentre distances of the bins. Here, the bins are created uniformly, and thus $F(r) \propto r^{[\sim(1-q)]} \propto r^{(-0.65)}$. The bottom-right panel shows the properties of line intensities ($f_{i,j}$) of the 23 541 data points in 60 elliptical rings with pericentre distances from r_0 to r_1. The bottom two panels show the properties of equation (2).

$f_{i,j}(i = 1...N, j = 1...M)$ can be directly calculated using the elliptical accretion disc model. The total line intensity F is the sum of $f_{i,j}$:

$$f_{i,j} = \int_{r_{\star,i}}^{r_{\star,i+1}} \int_{\phi_j}^{\phi_{j+1}} H(\text{model})\, \mathrm{d}r\, \mathrm{d}\phi \propto P(r_i, \phi_j)$$

$$\sum_j f_{i,j} = F_i \propto r_{\star,i}^{q_\star}$$

$$\sum_i \sum_j f_{i,j} = F. \tag{2}$$

Here, H(model) is the integrand function used for the accretion disc model (as shown in Eracleous et al. 1995). $q_\star$ is different from the emissivity slope in the elliptical accretion disc model (however, if the radius of each bin is uniformly created, then $q_\star \sim 1.0 - q$, as shown in Fig. 6). $P(r_i, \phi_j)$ is the function, depending on the radius and orientation angle, used to calculate the line intensity of each tiny cloud in the ith elliptical ring, which can also be found in Fig. 6. F_i and F are the line intensity from the ith elliptical ring and the total line intensity from the total area, respectively. Here, we select $N = 60$ and $M = 400$. $N = 60$ confirms that the light travel time from the ith bin to the $i + 1$th bin is much less than 1 d (especially for the bins in the inner part of the BLRs), the standard date separation of our input light curve of continuum emission. Furthermore, we should note that, in our procedure, the listed disc parameters above are taken as fixed values, based on the following considerations. On the one hand, there are tiny variations of the line profiles of double-peaked Hα observed around 1995. Based on the observed Hα selected from the AGN Watch project, it is very difficult to find one reliable correlation between the line profile variability and the disc parameters (especially the orientation angle ϕ) using the theoretical disc model. In other words, there is no information about the function of $\phi(t)$, where t is the date and time. On the other hand, the fixed disc parameters, through tiny varied line profiles, around 1995 lead to a much simpler mathematical procedure.

Fig. 6 shows the procedures above used to build the structures of the BLRs of 3C 390.3 based on the disc parameters, including the properties of equation (2). Once a tiny cloud meets the ionizing photon from the central source, the line intensity of the tiny cloud is changed immediately to

$$f_{i,j}(t) \propto f_{i,j}(t-1) \left(\frac{con_{i,j}(t)}{con_{i,j}(t-1)} \right)^{\alpha}. \tag{3}$$

Here, t is the date with the uniform separation of 1 d as discussed below, α is the slope of the corresponding correlation between the luminosity of Hα and the continuum luminosity, and $f_{i,j}$ and $con_{i,j}$ are the line intensity from area $A(i, j)$ and the arriving continuum emission for area $A(i, j)$, respectively. For AGNs, α is about 1 for quasi-stellar objects (QSOs) in Greene & Ho (2005), and for low-luminosity AGNs in Zhang, Dultzin & Wang (2008). However, $\alpha \sim 1$ is not preferred for 3C 390.3. Fig. 7 shows the correlation between the continuum luminosity at 5177 Å and the luminosity of broad Hα for the spectra observed around 1995. The values of the luminosity of broad Hα and continuum luminosity at 5177 Å are collected from the AGN Watch project, and the contamination has been corrected. The Spearman rank correlation coefficient is about 0.66 with $P_{null} \sim 10^{-9}$. Using the Levenberg–Marquardt least-squares minimization technique, the best-weighted fitted result for the correlation can be

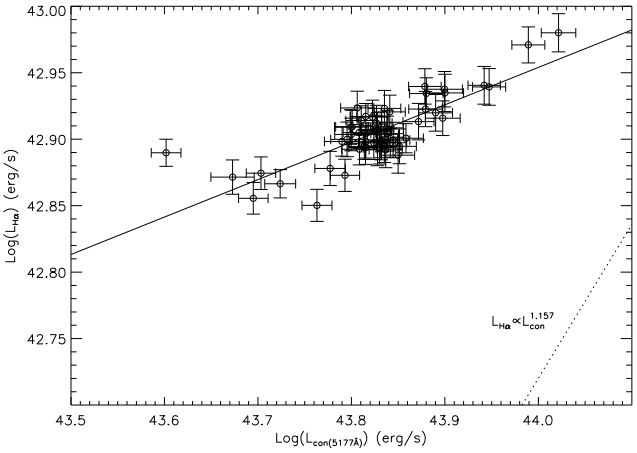

Figure 7. The correlation between the luminosity of broad Hα and the continuum luminosity at 5177 Å for the 66 spectra observed around 1995. The solid line represents the best-fitting result, $L_{H\alpha} \propto [L_{\mathrm{con}(5177\,\text{Å})}]^{0.265}$. The dotted line is the one found by Greene & Ho (2005).

calculated as

$$L_{H\alpha} = 8.92 \times 10^{42} \left(\frac{L_{\mathrm{con}(5177\,\text{Å})}}{10^{44}\,\mathrm{erg\,s^{-1}}} \right)^{0.26\pm0.03} \quad \mathrm{erg\,s^{-1}}. \tag{4}$$

Thus, we accept $\alpha \sim 0.26$, not $\sim$1. Actually, the different index of the line–continuum luminosity correlation is because of the contamination of narrow lines around Hα. As shown in Dietrich et al. (1998), the flux density of broad Hα includes contributions from narrow lines around Hα, and flux densities of narrow emission lines are constant for 3C 390.3. If we define factor k as the flux ratio of pure broad Hα to narrow lines, we should find that points with lower luminosity of Hα in Fig. 7 have smaller values of k; points with larger luminosity of Hα in Fig. 7 have larger values of k. If the contributions of narrow emission lines are corrected, the index for the correlation shown in Fig. 7 should be steeper than 0.26 and near to 1.

Fig. 8 shows one simple output line curve of broad Hα based on one test input light curve of continuum emission described by one delta function through the disc-like BLRs determined using the elliptical accretion disc model for 3C 390.3. Because of the extended BLRs, the delta function is delayed and expanded. Light travelling from the central BH (we assume that the ionizing photons are from central point) to the innermost boundary of the BLRs is about 5 d, from the inner boundary ($\sim 216 R_{\mathrm{G}}$) to the point with the longest distance ($\sim 1640 R_{\mathrm{G}}$, larger than the pericentre distance $1263 R_{\mathrm{G}}$ for the outer boundary, because the BLRs are elliptical disc-like) from the central BH is about 39 d. Thus, in Fig. 8, it is clear that 5 d after the burst of continuum, the line intensity starts to vary. Then, 39 d after the burst of continuum emission, the variation of line intensity ends. Because the inner part of the BLRs emits most of the line intensity of broad Hα, the line intensity of total Hα is changed from strong to weak with the passage of time, as shown in Fig. 8. Furthermore, it should be interesting to check the effects of the different geometrical structure on the response output of broad Hα, although in the previous section we have accepted that there are fixed and stable disc parameters. We accepted the disc parameters for 3C 390.3 under the stochastically perturbed accretion disc model in Flohic & Eracleous (2008) – one circular disc part with bright spots – $r_0 = 450 R_{\mathrm{G}}$, $r_1 = 1400 R_{\mathrm{G}}$, $\sigma = 1300\,\mathrm{km\,s^{-1}}$, $i = 27^o$ and $q = 3$, in spite of the not well fitted results for line profiles with these parameters (not good fitted results for broad wings). Under the model, the

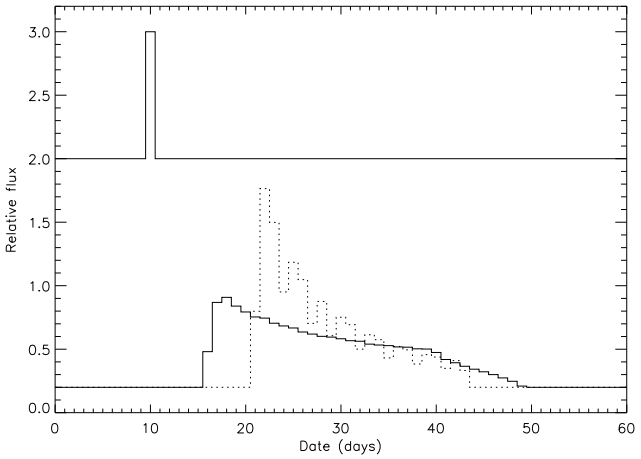

Figure 8. The response output broad Hα based on the input continuum emission described by one delta function under the elliptical disc-like BLR and circular disc-like BLR for 3C 390.3. The top line shows the continuum emission. The bottom solid line shows the corresponding response output broad Hα under the elliptical disc-like BLR and the dotted line shows the results under the circular disc-like BLR.

output Hα is also shown in Fig. 8. It is clear that the response to input continuum described delta function is very different for the elliptical disc and circular disc structures. The different responses for the different geometrical structures indicate that the different structures of the BLRs of AGNs should be discriminated using the light curves of continuum emission and broad emission-line emission, especially when there is homogeneous and complete information for the light curves. Actually, based on the observed light curves of 3C 390.3 selected from the AGN Watch project, there is no way to discriminate between the different geometrical structures of the BLRs, as we show in the following results. The results shown in Fig. 8 indicate that our procedures do work, and the effects of extended disc-like BLRs on the light curve of the emission line can be clearly described by our procedures.

Last but not least, the observed light curve of the continuum emission at $\sim$5177 Å, collected from the AGN Watch project, is used as the input light curve of the continuum emission. A detailed description of the light curve can be found in Dietrich et al. (1998). There are 70 data points included in the light curve from MJD 244 9517 to MJD 245 0068. We first create one new light curve of continuum emission with a date separation of 1 d using the linear interpolation method applied to the observed light curve of continuum. Then, we check the expected output light curve of broad Hα under the supposed elliptical disc-like BLRs. The results are shown in bottom-left panel of Fig. 9. It is clear that the expected output light curve of broad Hα is consistent with the observed light curve of broad Hα. The linear correlation coefficient for the correlation between the output light curve of Hα and the observed light curve of Hα is about 0.85 with $P_{null} \sim 0$. Then, using the input light curve of continuum and the output corresponding light curve of broad Hα, it is interesting to estimate the size of BLRs using the so-called CCF. Here, the common interpolated cross-correlation function (ICCF) (Gaskell & Sparke 1986; Gaskell & Peterson 1987; Peterson 1993) is applied to quantify the time lag between the continuum emission and broad-line emission. We no longer consider the z-transfer

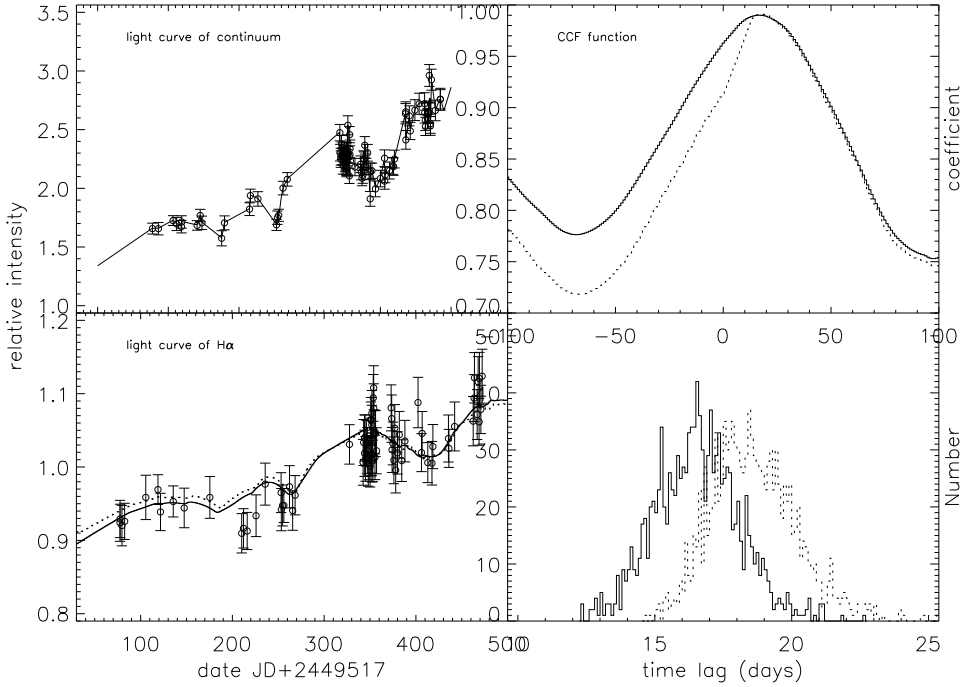

Figure 9. The top-left panel shows the light curve of the continuum: open circles are the observed data points selected from the AGN Watch project and the solid line represents the input light curve of the continuum with a separation of 1 d. The bottom-left panel shows the light curve of broad Hα: open circles are the observed values, the solid line represents the output light curve under the elliptical disc-like BLRs and the dotted line represents the output light curve under the circular disc model, as shown in Flohic & Eracleous (2008). The top-right panel shows the CCF function (maximum coefficient about 0.99) for the observed light curve of continuum emission and the output light curve of broad Hα. The solid line represents the result for the elliptical accretion disc model (peak value around 16 d) and the dotted line shows the result for the circular disc model in Flohic & Eracleous (2008) (peak value around 18 d). The bottom-right panel shows the distribution of time lag between the observed continuum emission and the broad Hα emission simulated using the bootstrap method. The solid line is for the elliptical disc model and the dotted line is for the circular disc model in Flohic & Eracleous (2008).

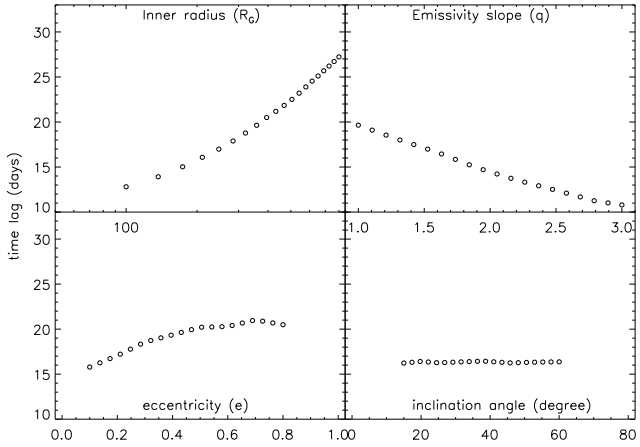

Figure 10. The effects of disc parameters on the theoretically measured size of BLRs. The top-left panel shows the effects of inner radius, the top-right panel shows the effects of emissivity power, the bottom-left panel shows the effects of eccentricity and the bottom-right panel shows the effects of inclination angle.

discrete correlation function (ZDCF; Edelson & Krolik 1988; White & Peterson 1994; Alexander 1997) because the results from the ZDCF are in excellent agreement with the results from the ICCF (Peterson et al. 1991, 1992, 2004; Kaspi et al. 2000; Bentz et al. 2010). Furthermore, the corresponding results based on the disc parameters shown in Flohic & Eracleous (2008) are also calculated, and are shown in Fig. 9. It is clear that, although the example shown in Fig. 8 indicates that the information from light curves can be used to confirm which structure should be more preferred, there is no way to find enough evidence to determine which structure (elliptical disc-like BLR or circular disc-like BLR) is preferred, because of the incomplete and inhomogeneous information provided by the observed light curves. Thus, we mainly compare the calculated time lags between the continuum emission and broad-line emission, under the two structures.

Fig. 9 shows the CCF results from the input light curve of continuum and the output light curve of broad Hα, the distribution of the size of BLRs using the bootstrap method (a common Monte Carlo method to estimate the uncertainty of parameters; Press et al. 1992; Peterson et al. 1998). Detailed descriptions about the CCF method used to estimate the size of BLRs (the time lag between line emission and continuum emission) and the bootstrap method used to estimate the uncertainties of measured time lag can be found in Peterson (1993). From the results shown in the figure, we can find that the estimated size of the BLRs using the input light curve of continuum emission and output light curve of broad Hα with the elliptical accretion disc model is also very consistent with that estimated by the observed light curves of continuum emission and broad-line emission, $R_{\rm BLRs} \sim 16.8 \pm 2.1$ light-days. We should note that the size of BLRs is the distance from the broad Hα emission-line region to the optical continuum emission region. Thus, the value is smaller than the ∼20 light-days estimated by the CCF function from the light curve of broad Hα and the light curve of X-ray/UV emission shown in Dietrich et al. (1998), Bentz et al. (2009), etc., because there is probably a 5-d lag between the optical continuum emission and the X-ray emission (Dietrich et al. 1998). Certainly, we also calculate the results based on the circular disc model shown in Flohic & Eracleous (2008), which should be different from the results for the elliptical accretion disc model, $R_{\rm BLRs} \sim 18.4 \pm 2.1$ light-days. However, there is not enough evidence against the circular disc-like BLR for 3C 390.3, besides the best-fitting results for the observed line profiles. If there were homogeneous and complete observed light curves, a clear final decision could be given.

In order to further confirm that the disc-like BLRs determined by the elliptical accretion disc model are reliable for the double-peaked emitter 3C 390.3, we also check the CCF results for disc-like BLRs with different disc parameters, in spite of the best-fitting results for the observed double-peaked broad Balmer line. Fig. 10 shows the effects of the disc parameters on the measured size of BLRs through input continuum emission and output Hα emission, based on the elliptical accretion disc model, as we have done above. It is clear that the inner radius and emissivity power are the two main parameters that have apparent effects on the theoretically measured size of the BLRs of 3C 390.3. In the figure, we only show the effects from the inner radius, emissivity power, eccentricity and inclination angle of the disc-like BLRs, because there are few effects from the other disc parameters. Certainly, more reliable evidence to determine and confirm model parameters should depend on future more detailed and homogeneous observed light curves of continuum emission and broad-line emission. The results indicate that the measured disc parameters for the BLRs of 3C 390.3 are reliable to some extent, and the different geometrical structures of the BLRs based on different disc parameters should lead to different sizes for BLRs measured theoretically and obtained using observations.

The results above indicate that the elliptical accretion disc model can be applied to best fit the observed spectra (i.e. the model can provide fine velocity structures for the BLRs of 3C 390.3). Furthermore, the elliptical accretion disc model can provide fine geometrical structures, which can be applied to reproduce the characteristics of the observed light curve of broad Hα. Thus, the elliptical accretion disc model, which can be applied to fit the characteristics of line profiles and variations of broad double-peaked Hα, is appropriate for the double-peaked emitter 3C 390.3.

4 DISCUSSION AND CONCLUSION

Based on the disc parameters measured above, it is very interesting to check the expected line profile of the double-peaked broad Balmer emission line of 3C 390.3, a well-known double-peaked emitter, for different years/periods. Although the more recent observed line profiles of the double-peaked broad Hα of 3C 390.3 in 2007 January can be found in Shapovalova et al. (2010), the spectrum observed in 2000 September by the *Hubble Space Telescope* (*HST*) STIS is used, because the reduced spectrum in 2000 is public and can conveniently be collected from the website of the Multimission Archive at the Space Telescope Science Institute (MAST)[2] (*HST* Proposal 8700, PI: Professor Andre Martel, Space Telescope Science Institute). A detailed description about the observational technique for the spectrum observed around 2000 by the *HST* can be found in Popovic (2003). Here, we mainly check whether the observed line profile of broad Balmer emission lines in 2000 can be reproduced using the theoretical elliptical accretion disc model, based on the disc parameters measured from spectra observed around 1995 for the double-peaked emitter 3C 390.3.

Before proceeding further, the precession period should be determined. Using the obtained disc parameters, the relativistic

[2] See http://archive.stsci.edu/

precession period of the elliptical disc-like BLRs around the central BH of 3C 390.3 can be simply calculated (Weinberg 1972):

$$T_{\rm pre} = \frac{2\pi}{\delta_\phi} \sim (2\pi)\left[\frac{6\pi G M_{\rm BH}}{c^2 A(1-e^2)}\right]^{-1} \sim 70\,{\rm yr} \quad ({\rm inner\,radius}) \sim 370\,{\rm yr} \quad ({\rm outer\,radius}). \tag{5}$$

Here, A is the semimajor axis length and e is the eccentricity. Although the precession period for the outer elliptical rings is very long, the short precession period for the inner elliptical rings should lead to some apparent variations of the double-peaked broad emission lines from 1995 to 2000.

We simply assume that the orientation angle is the unique parameter to vary from 1995 to 2000 in the elliptical accretion disc model. As we have done in Section 3, the elliptical disc-like BLRs are separated into 60 rings. It is clear that orientation angle of each ring in 2000 should be different because of the different semimajor axis length for each ring, $\phi_{2000,i} = \phi_{1995,i} \pm 2\pi(5/T_{{\rm pre},i})$, where $\pm$ means that the rotating direction of the disc-like BLRs is clockwise or anticlockwise for the observer. After the orientation angles of the 60 rings around 2000 are determined, the line profile expected in 2000 can be reconstructed using the sum of the 60 expected double-peaked components from the 60 rings, as we have done in Section 3. Here, the theoretical line profile in 2000 is mainly based on the mean spectrum around 1995 in the AGN Watch project. The mean observed spectrum (shown as a thin solid line in Fig. 11) is created by principal component analysis (PCA) method, the so-called Karhunen–Loeve transform, applied for all 66 observed spectra of broad Hα around 1995. The convenient and public IDL PCA program 'pca_solve.pro' written by D. Schlegel at Princeton University is used. This is included in the Sloan Digital Sky Survey (SDSS) software package IDLSPEC2D.[3] Commonly, the first principal component represents the mean spectrum. From the mean spectrum, it is clear that the flux ratio ($\sim$1.46) of blue peak to red peak for broad double-peaked Hα and the flux ratio ($\sim$1) of blue part to red part are similar to the mean values shown in Fig. 4.

Fig. 11 shows the probable line profile of broad double-peaked Hα of 3C 390.3 observed around 2000. It also shows a comparison between the mean spectrum observed around 1995 and the spectrum observed around 2000. Based on the theoretical accretion disc model, using the results shown in the top-left panel of Fig. 11, we find that because of the precession period, after about 5 yr, the flux ratio of the red peak to blue peak should be changed. In the figure, the flux density at the blue peaks of all the line profiles have been normalized to 1. If the rotating direction of disc-like BLRs is clockwise to the observer, the expected flux ratio (1.36) of the red peak to blue peak of the spectrum around 2000 should be smaller than that of the spectrum observed around 1995 (1.46). If the rotating direction of the disc-like BLRs is anticlockwise to the observer, the expected flux ratio (1.68) in 2000 should be larger than that (1.46) in 1995. Using the spectrum observed in 2000, the flux ratio of the blue peak to red peak is about 1.79 ± 0.18. Thus, if anticlockwise rotating disc-like BLRs are applied to 3C 390.3, the variations in the spectra observed in different years can naturally be explained, although the applied model is oversimplified. The larger value of 1.79 compared with the theoretical expected value of 1.68 is perhaps a result of the not so accurate precession period, the probable

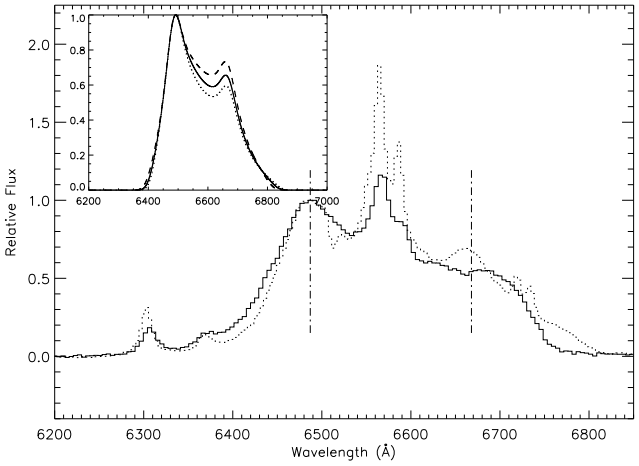

Figure 11. A comparison of the line profile observed by *HST* in 2000 and the mean line profile observed around 1995. The thin dotted line represents the mean spectrum around 1995 and the thick solid line represents the line profile observed by *HST* in 2000. The two vertical dot-dashed lines mark the positions of the red peak and blue peak of the double-peaked broad Hα. The top-left panel shows the theoretical results. The solid line represents the mean double-peaked line profile observed around 1995, the thick dashed line represents the line profile expected around 2000 with clockwise rotating disc-like BLRs and the thick dotted line represents the line profile expected around 2000 with anticlockwise rotating disc-like BLRs.

existence of varying of hotspots and/or warped structures, the different local broadening velocity (which should lead the part around the red peak to be flat), etc. The not so consistent red peak positions for the spectrum around 2000 and the mean spectrum around 1995 are probably a result of the variation of the emissivity power slope during the 5 yr from 1995 to 2000.

Finally, a simple summary is listed as follows. Based on the spectra observed around 1995 for 3C 390.3, the elliptical accretion disc model is applied to fit the observed double-peaked broad Hα collected from the AGN Watch project. Then, based on the disc parameters, the formed geometrical structures of the BLRs of 3C 390.3 are applied to check the reverberation mapping results for 3C 390.3. The disc-like BLRs supposed by the theoretical elliptical accretion disc model can reproduce well the observational results about the reverberation mapping technique. Thus, disc-like BLRs are preferred for 3C 390.3. Furthermore, we check the effects of the precession of elliptical disc-like BLRs on the observed line profile. After about 5 yr, the line profile of broad double-peaked Hα observed in 2000 by *HST* can be well predicted by the theoretical elliptical accretion disc model, based on the disc parameters measured using spectra observed around 1995. This confirms that the elliptical accretion disc model is appropriate for the double-peaked emitter 3C 390.3.

ACKNOWLEDGMENTS

XGZ gratefully acknowledges the anonymous referee for providing constructive comments and suggestions, which have greatly improved the paper. XGZ gratefully acknowledges financial support from Chinese grant NSFC-11003034, and useful discussions with Professor Ting-Gui Wang of the University of Science and Technology of China (USTC). We are grateful to the AGN Watch project (http://www.astronomy.ohio-state.edu/~agnwatch/) for making it convenient for us to collect the spectra of 3C 390.3. We thank Professor Andre Martel of the Space Telescope Science Institute, who

[3] See http://spectro.princeton.edu/

provided the public *HST* spectra of 3C 390.3. We are grateful for the use of MAST, which is a project funded by the National Aeronautics and Space Administration (NASA) to support the astronomical community and to provide a variety of astronomical data archives, with the primary focus on scientifically related data sets in the optical, UV and near-infrared parts of the spectrum. We are grateful for the public SDSS IDL code provided by Dr David Schlegel of Princeton University, and the public Markwardt IDL library. This research has made use of the NASA/IPAC Extragalactic Data base (NED), which is operated by the Jet Propulsion Laboratory, California Institute of Technology, under contract with NASA.

REFERENCES

Alexander T., 1997, in Maoz D., Sternberg A., Leibowitz E. M., eds, Astronomical Time Series. Kluwer, Dordrecht, p. 163
Bachev R., 1999, A&A, 348, 71
Begelman M. C., Blandford R. D., Rees M. J., 1980, Nat, 287, 307
Bentz M. C., Peterson B. M., Pogge R. W., Vestergaard M., Onken C. A., 2006, ApJ, 644, 133
Bentz M. C., Peterson B. M., Netzer H., Pogge R. W., Vestergaard M., 2009, ApJ, 697, 160
Bentz M. C. et al., 2010, ApJ, 720, L46
Blandford R. D., Mckee C. F., 1982, ApJ, 255, 419
Boroson T. A., Lauer T. R., 2009, Nat, 458, 53
Brandon C. K., Bechtold J., 2007, ApJS, 168, 1
Chen K. Y., Halpern J. P., 1989, ApJ, 344, 115
Chen K. Y., Halpern J. P., Filippenko A. V., 1989, ApJ, 339, 742
Chornock R. et al., 2010, ApJ, 709, 39
Collin S., Kawaguchi T., Peterson B. M., Vestergaard M., 2006, A&A, 456, 75
Dietrich M. et al., 1998, ApJS, 115, 185
Edelson R. A., Krolik J. H., 1988, ApJ, 333, 646
Eracleous M., Halpern J. P., 1994, ApJS, 90, 1
Eracleous M., Halpern J. P., 2003, ApJ, 599, 886
Eracleous M., Livio M., Halpern J. P., Storchi-Bergmann T., 1995, ApJ, 438, 610
Eracleous M., Halpern J. P., Gilbert A. M., Newman J. A., Filippenko A. V., 1997, ApJ, 490, 216
Eracleous M., Lewis K. T., Flohic H. M. L. G., 2009, New Astron. Rev., 53, 133
Ferrarese L., Merritt D., 2001, MNRAS, 320, L30
Flohic H. M. L. G., Eracleous M., 2008, ApJ, 686, 138
Gaskell C. M., 1983, in Proc. 24th Liege International Astrophysical Colloquium, Quasars and Gravitational Lenses. Universite de Liege, Cointe-Ougree, Belgium, p. 473
Gaskell M., 1996, ApJ, 464, 107
Gaskell C. M., 2010, Nat, 463, 1
Gaskell C. M., Peterson B., 1987, ApJS, 65, 1
Gaskell C. M., Sparke L. S., 1986, ApJ, 305, 175
Gebhardt K. et al., 2000, ApJ, 539, L13
Gezari S., Halpern J. P., Eracleous M., 2007, ApJ, 169, 167
Goad M. R., O'Brien P. T., Gondhalekar P. M., 1993, MNRAS, 263, 149
Greene J. E., Ho L. C., 2005, ApJ, 630, 122
Göltekin K. et al., 2009, ApJ, 698, 198
Halpern J. P., 1990, ApJ, 365, L51
Hartnoll S. A., Blackman E. G., 2000, MNRAS, 317, 880
Hartnoll S. A., Blackman E. G., 2002, MNRAS, 332, L1
Horne K., Welsh W. F., Peterson B. M., 1991, ApJ, 367, L5
Jovanovic P., Popovic L. C., Stalevski M., Shapovalova A. I., 2010, ApJ, 718, 168
Karas V., Martocchia A., Subr L., 2001, PASJ, 53, 189
Kaspi S., Smith P. S., Netzer H., Maoz D., Jannuzi B. T., Giveon U., 2000, ApJ, 533, 631
Kaspi S., Maoz D., Netzer H., Peterson B. M., Vestergaard M., Jannuzi B. T., 2005, ApJ, 629, 61
Krolik J. H., 1994, in Courvoisier T. J.-L., Blecha A., eds, Proc. IAU Symp. 159, Multiwavelength Continuum Emission of AGN. Kluwer, Dordrecht, p. 163
Lauer T. R., Boroson T. A., 2009, ApJ, 703, 930
Leighly K. M., O'Brien P. T., Edelson R., George I. M., Malkan M. A., Matsuoka M., Mushotzky R. F., Peterson B. M., 1997, ApJ, 483, 767
Lewis K. T., Eracleous M., 2006, ApJ, 642, 711
Lewis K. T., Eracleous M., Storchi-Bergmann T., 2010, ApJS, 187, 416
Livio M., Xu C., 1997, ApJ, 478, L63
Maoz D., 1996, in Peterson B. M., Cheng F-Z., Wilson A. S., eds, ASP Conf. Ser. Vol. 113, Emission Lines in Active Galaxies: New Methods and Techniques. Astron. Soc. Pac., San Francisco, p. 138
Merritt D., Ekers R. D., 2002, Sci, 297, 1310
Narayan R., Nityananda R., 1986, ARA&A, 24, 127
O'Brien P. T. et al., 1998, ApJ, 509, 163
Oke J. B., 1987, in Zensus J. A., Pearson T. J., eds, Superluminal Radio Sources. Cambridge Univ. Press, Cambridge, p. 267
Onken C. A., Ferrarese L., Merritt D., Peterson B. M., Pogge R. W., Vestergaard M., Wandel A., 2004, ApJ, 615, 645
Perez E., Penston M. V., Tadhunter C., Mediavilla E., Moles M., 1988, MNRAS, 230, 353
Peterson B. M., 1993, PASP, 105, 247
Peterson B. M., 2010, in Peterson B., Somerville R., Storchi-Bergmann T., eds, Proc. IAU Symp. 267, Co-Evolution of Central Black Holes and Galaxies. Kluwer, Dordrecht, p. 151
Peterson B. M., Bentz M. C., 2006, New Astron. Rev., 50, 796
Peterson B. M. et al., 1991, ApJ, 368, 119
Peterson B. M. et al., 1992, ApJ, 392, 470
Peterson B. M., Ali B., Horne K., Bertram R., Lame N. J., Pogge R. W., Wagner R. M., 1993, ApJ, 402, 469
Peterson B. M. et al., 1994, ApJ, 425, 622
Peterson B. M., Wanders I., Horne K., Collier S., 1998, PASP, 110, 660
Peterson B. M. et al., 2004, ApJ, 613, 682
Pijpers F. P., Wanders I., 1994, MNRAS, 271, 183
Popovic L. C., 2003, ApJ, 599, 140
Press W. H., Teukolsky S. A., Vetterling W. T., Flannery B. P., 1992, Numerical Recipes in Fortran 77, 2nd edn. Cambridge Univ. Press, Cambridge
Pronik V. I., Sergeev S. G., 2007, in Gaskell C. M., McHardy I. M., Peterson B. M., Sergeev S. G., eds, Proc. ASP Conf. Ser. Vol. 360, AGN Variability from X-Rays to Radio Waves. Astron. Soc. Pac., San Francisco, p. 231
Sambruna R. M. et al., 2009, ApJ, 700, 1473
Sergeev S. G., Pronik V. I., Peterson B. M., Sergeeva E. A., Zheng W., 2002, ApJ, 576, 660
Shapovalova A. I. et al., 2001, A&A, 376, 775
Shapovalova A. I. et al., 2010, A&A, 517, 42
Stauffer J., Schild R., Keel W., 1983, ApJ, 270, 465
Storchi-Bergmann T., Eracleous M., Livio M., Wilson A. S., Filippenko A. V., Halpern J. P., 1995, ApJ, 443, 617
Storchi-Bergmann T., Eracleous M., Ruiz M. T., Livio M., Wilson A. S., Filippenko A. V., 1997, ApJ, 489, 87
Storchi-Bergmann T. et al., 2003, ApJ, 598, 956
Strateva I. V. et al., 2003, AJ, 126, 1720
Tran H. D., 2010, ApJ, 711, 1174
Tremaine S. et al., 2002, ApJ, 574, 740
van Groningen E., Wanders I., 1992, PASP, 104, 700
Veilleux S., Zheng W., 1991, ApJ, 377, 89
Wanders I., Horne K., 1994, A&A, 289, 76
Weinberg S., 1972, Gravitation and Cosmology. Wiley, New York, p. 185
White R. J., Peterson B. M., 1994, PASP, 106, 876
Winge C., Peterson B. M., Horne K., Pogge R. W., Pastoriza M., Storchi-Bergmann T., 1995, ApJ, 445, 680
Woo J. H. et al., 2010, ApJ, 716, 269
Zhang X. G., Dultzin D., Wang T. G., 2007, MNRAS, 377, 1215
Zhang X. G., Dultzin D., Wang T. G., 2008, MNRAS, 385, 1087
Zheng W., Sulentic J. W., Binette L., 1990, ApJ, 365, 115
Zheng W., Veilleux S., Grandi S. A., 1991, ApJ, 381, 418

This paper has been typeset from a TEX/LATEX file prepared by the author.